

## Self-Diffusivity in Block Copolymer Solutions. 2. A<sub>2</sub>B Simple Grafts

S. H. Anastasiadis,<sup>\*,†</sup> K. Chrissopoulou, and G. Fytas

Foundation for Research and Technology—Hellas, Institute of Electronic Structure and Laser, P.O. Box 1527, 711 10 Heraklion Crete, Greece

G. Fleischer

Universität Leipzig, Fakultät für Physik und Geowissenschaften,  
D-04103 Leipzig, Germany

S. Pispas, M. Pitsikalis, and J. W. Mays

University of Alabama at Birmingham, Department of Chemistry,  
Birmingham, Alabama 35294

N. Hadjichristidis<sup>‡</sup>

University of Athens, Department of Chemistry, Zografou University City,  
157 01 Zografou, Athens, Greece

Received November 26, 1996; Revised Manuscript Received January 31, 1997<sup>®</sup>

**ABSTRACT:** The composition and concentration dependencies of the self-diffusion coefficients for a series of miktoarm star block copolymers of the A<sub>2</sub>B type in solutions in a common good solvent have been investigated by pulsed-field-gradient nuclear magnetic resonance; the graft copolymers are composed of A = polyisoprene and B = polystyrene, where the B block was attached either in the middle of the A block ( $\tau = 0.5$ ) or at a position with  $\tau = 0.25$ . The dependence of the diffusion coefficients on concentration, in both A<sub>2</sub>B graft copolymers and AB diblock copolymers, can be collapsed onto a master curve with a proposed scaling procedure which takes into account the difference in the entanglement characteristics of the parent homopolymers and the different radii of gyration of stars vs linear polymers. The exponential slowing down of the diffusivities expected for star molecules was not observed due to the only moderately high molecular weights and concentrations.

### 1. Introduction

The rich variety of phase behavior of block copolymers has attracted scientific interest over several years;<sup>1</sup> the thermodynamic incompatibility between the covalently bonded linear sequences of chemically different monomers leads to a disorder-to-order transition<sup>2</sup> (ODT) from a homogeneous or disordered state at low enough values of  $\chi N$  toward a microphase-separated state characterized by long-range order in its composition at higher  $\chi N$  values.  $N$  is the overall degree of polymerization, and  $\chi$  the segment-segment Flory–Huggins interaction parameter ( $\chi = a + b/T$  with  $b > 0$ ), whereas the phase state depends on  $f$ , the volume fraction of the A block, as well. The effects of the molecular architecture on the static behavior have also been considered<sup>3–5</sup> in recent years, where going from diblocks to graft, triblock, and star copolymers increases their compatibility (i.e., increases the effective  $\chi N$  at the transition). Solutions in neutral good solvents have long been used to complement the investigations on diblock copolymers,<sup>6,7</sup> where the unfavorable interactions between the blocks are diluted by the solvent, and the disordered state may be investigated even for high molecular weight copolymers.

In contrast, the dynamic behavior of block copolymers (and especially diblocks) has only recently attracted a

great deal of interest.<sup>8,9</sup> Experimental investigations<sup>9</sup> were concerned with the linear and nonlinear viscoelastic properties of diblock copolymers, as well as with the mechanisms of relaxation of composition and orientation fluctuations and the diffusion in both disordered and ordered diblocks in the melt and in semidilute solutions; they have utilized a variety of techniques like dynamic light scattering, forced Rayleigh scattering, forward recoil spectroscopy, and pulsed-field-gradient nuclear magnetic resonance (PFG-NMR). Theories, at the same time, were developed<sup>9</sup> to predict the rheology of disordered diblock melts, to derive the intermediate scattering function and its relaxation characteristics, and to investigate the translational diffusivities in both weakly and strongly ordered diblock copolymer melts.

Significant effort was devoted to the study of the self- and tracer-diffusion in both disordered and ordered diblock copolymers in the melt and in solution. The aim was to understand the influence of thermodynamic and entanglement constraints on the diffusivities. The diffusion coefficients conformed to the  $D \sim N^{-1}$  Rouse dynamics scaling for disordered melts of low molecular weight diblocks,<sup>10</sup> and showed little sensitivity to the crossing of the ODT.<sup>10–12</sup> For high molecular weight entangled diblocks, the diffusivities exhibited the  $D \sim N^{-2}$  reptation scaling in the disordered state<sup>13</sup> and a smooth temperature dependence through the ODT,<sup>10,13,14</sup> whereas the chains were significantly retarded in the ordered state.<sup>10</sup> The weak sensitivity of the diffusivities on crossing the ODT was also observed for diblock copolymer solutions.<sup>15,16</sup> Investigation of the mechanisms of chain diffusion in symmetric diblock copolymers indicated<sup>17</sup> that the diffusion in the lamellar plane

\* Author to whom correspondence should be addressed.

<sup>†</sup> Also at University of Crete, Physics Department, 710 03 Heraklion Crete, Greece.

<sup>‡</sup> Also at Foundation for Research and Technology—Hellas, Institute of Electronic Structure and Laser, P.O. Box 1527, 711 10 Heraklion Crete, Greece.

<sup>®</sup> Abstract published in *Advance ACS Abstracts*, March 15, 1997.

occurred by an activated reptation process for entangled diblocks near ODT ( $8 < \chi N < 20$ ) and a crossover to an entropic block retraction mechanism at higher  $\chi N$ s, whereas a thermodynamic barrier was found to affect the diffusion through the layers as well.

An investigation of the coupling of thermodynamic and entanglement constraints in the disordered state was also attempted in previous investigations from this laboratory,<sup>18,19</sup> where the composition,  $f$ , and concentration,  $\phi$ , dependence of the self diffusion coefficients of diblock copolymers in solution in a common good solvent were investigated by PFG-NMR and photon correlation spectroscopy (PCS). The diffusivities were found to be significantly influenced by the entanglement characteristics of the parent homopolymers. For toluene solutions of polystyrene–polybutadiene<sup>18</sup> and polystyrene–polyisoprene<sup>19</sup> diblocks with similar molecular weights but varying compositions, the significant variation of the self diffusion coefficients as a function of  $f$  for every  $\phi$  was appreciably reduced when  $\phi$  was reduced by the concentration  $\phi_e$  where entanglement effects should become important ( $\phi_e$  depends on  $f$  due to the vastly different bulk entanglement characteristics of the parent homopolymers). Concurrently, the self-diffusivities of polystyrene–poly(methyl methacrylate) diblocks with similar molecular weights in toluene were insensitive to composition<sup>19</sup> in accord with the very similar entanglement characteristics of the parent homopolymers.

Macromolecular architecture is expected to significantly influence the dynamic behavior of nonlinear (like star-branched) molecules vs linear ones. As will be discussed in section 2, the severe restrictions on the chain motion especially in the entanglement regime<sup>20</sup> can significantly retard the dynamics, leading to an exponential increase of the viscosity and the concurrent exponential slowing down of the longest relaxation time and the self-diffusion coefficient relative to the respective linear polymers. On the other hand, in the Rouse regime, the motion of a starlike macromolecule is influenced<sup>21</sup> by its smaller size relative to a linear one leading to smaller viscosities and faster relaxation times and diffusivities. At the same time, when discussing nonlinear block copolymers, the increased compatibility vs the respective diblocks may influence the effects of thermodynamics on the diffusivities<sup>10</sup> as well.

In this report, we present a pulsed-field-gradient nuclear magnetic resonance investigation on the composition,  $f$ , and concentration,  $\phi$ , dependence of the self-diffusion coefficients in toluene solutions for two series of (polyisoprene)<sub>2</sub>(polystyrene), I<sub>2</sub>S, miktoarm star block copolymers possessing similar molecular weights and compositions ranging from 0.11 to 0.92 in volume fraction of polyisoprene,  $f_{PI}$ . In one series, the polystyrene block was covalently bonded at the middle of the polyisoprene block ( $\tau = 0.5$ ) whereas in the second it was situated at a 25:75 position along the polyisoprene chain ( $\tau = 0.25$ ). Figure 1 shows a schematic of the molecular architecture of the I<sub>2</sub>S and the a-I<sub>2</sub>S grafts. The data are discussed in relation to the behavior in toluene solutions of linear polystyrene–polyisoprene diblocks of similar molecular weights and compositions to the I<sub>2</sub>S series. A dependence of the graft self-diffusion coefficients on composition for each concentration is observed with the rich in isoprene grafts being slower than the ones rich in styrene. The diffusivities of both A<sub>2</sub>B graft and AB diblock copolymers (even of different molecular weights) can be collapsed onto a master curve when plotted with an appropriate scaling that takes into account the difference in the entanglement character-

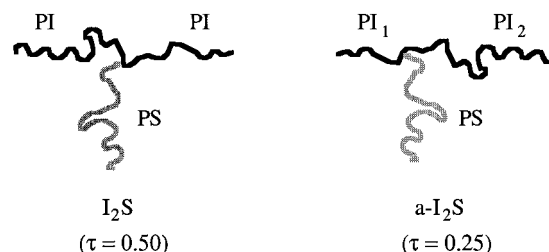


**Figure 1.** Schematic diagram of the I<sub>2</sub>S and a-I<sub>2</sub>S 3-miktoarm star copolymers. In the I<sub>2</sub>S series the polystyrene block is connected at the middle of the polyisoprene chain ( $\tau = 0.5$ ) whereas in the a-I<sub>2</sub>S series the polystyrene block is connected at a 25:75 position of the polyisoprene sequence ( $\tau = 0.25$ ).

istics of the parent homopolymers, the molecular weight, and the different radii of gyration of stars vs linear polymers. The exponential slowing down of the diffusivities expected and measured for entangled star homopolymers was not observed due to the modest molecular weights.

The remaining of this article is arranged as follows: Section 2 provides a short background on the dynamics and diffusion for star-branched homopolymers in solution. Following the Experimental Section, section 3, the results of the PFG-NMR investigations are presented and discussed in section 4, with the concluding remarks constituting section 5.

## 2. Dynamics of Star-Branched Homopolymers in Solution

The dynamics of multiarm homopolymer stars has attracted significant interest for many years, since they constitute a well-defined model system for the behavior of branched polymers; most of the effort<sup>22</sup> was devoted to the experimental<sup>22,23</sup> and theoretical<sup>20,21,24</sup> investigation of the viscoelastic properties of star-shaped polymers and less on their diffusional dynamics.<sup>25–30</sup> The major difference with linear homopolymers was established for the behavior in the well-entangled regime, i.e., when the molecular weight of each arm,  $M_a$ , was higher ( $>2–4$  times) than the molecular weight between entanglements,  $M_e$ . In this case, it has been postulated that motion of a star can only take place when an arm retracts to the position of the center monomer, without crossing any of the obstacles defining the reptation tube, and then moves out again; the probability of such folding back of the  $N_a$ -arm ( $N$ s stand for number of segments) was calculated<sup>20</sup> to be proportional to  $\exp(-\alpha N_a/N_e)$  for a three-arm star ( $\alpha$  is a constant) which leads to a similar exponential slowing down of the relaxation time (and, therefore, the viscosity) and the self-diffusivity. The possibility of a dependence of  $\alpha$  on the number of arms  $f_s$  of the star molecule ( $\alpha \propto f_s - 2$ ) is still a subject of discussion both on theoretical<sup>22b,24f,g</sup> and experimental<sup>30a</sup> grounds.

For lower arm molecular weights in the nonentangled Rouse regime, however, the viscosities of the star molecules are smaller than of linear chains of the same total molecular weight<sup>20</sup> because the coil size is smaller for the former; actually, the viscosities of stars both in melt and in solution superimpose with those of linear polymers when the molecular weight is scaled by the ratio  $g$

$$g = R_{g,br,0}^2 / R_{g,l,0}^2 \quad (1)$$

of the squares of the unperturbed radii of gyration of the branched ( $R_{g,br,0}$ ) and the linear ( $R_{g,l,0}$ ) polymer of the same total molecular weight. This means that in

the nonentangled regime, comparison of the dynamics of branched to that of linear molecules of the same molecular weight should be performed by using an effective number of segments for the star  $N_{\text{eff,star}} = gN$ ; this normalization is in agreement with the predictions that in the Rouse regime the zero shear viscosity of a star  $\eta_{\text{star}}^0 = g\eta_{\text{linear}}^0$  (note that  $\eta_{\text{linear}}^0 \propto N$ ).

The molecular weight between entanglements in solution is a function<sup>31</sup> of concentration,  $N_e(\phi) \cong N_e\phi^\beta$  with  $N_e$  the value in the bulk; experimentally,<sup>22c,31</sup>  $\beta \cong -1$  to  $-1.3$ , whereas theory predicts  $\beta = 1/(1 - 3\nu) \cong -1.30$  in the semidilute regime<sup>32,33</sup> ( $\nu$  is the Flory exponent,  $\nu \cong 0.59$  for good solvents) and  $\beta = -1$  for concentrated solutions<sup>33</sup> or recently<sup>34</sup>  $\beta = -1.25$ . As a result of this, the behavior at lower concentrations even for high arm molecular weights can be accounted for with the Rouse size reduction, whereas the viscosities of stars begin to increase rapidly at higher concentrations, with the viscosity enhancement factor exhibiting the exponential  $\exp[\alpha N_a/N_e(\phi)]$  dependence<sup>22a,23a</sup> discussed above; more precisely, data for different star polymers show an even better superposition when plotted<sup>22a,23a</sup> with respect to an  $\exp[\alpha\phi^{5/6}N_a/N_e(\phi)]$  dependence with  $\beta = -1$ . When one of the arms in a three-arm star is of a different length, one may have to think in terms of comb molecules; for model combs of  $p$  equidistant branches, the observed enhancement correlates<sup>35</sup> with the average end-to-end molecular weight of the comb, which for  $p = 1$  is simply  $^{2/3}$  of the total molecular weight.

The self-diffusion coefficient for homopolymer stars has been investigated both in the melt and in solution. For an entangled melt, theory predicts  $D \propto N_a^{-s} \exp(-\alpha N_a/N_e)$ ; however, the estimated<sup>20,24,28</sup> values for the exponent  $s$  vary over a broad range from 0.6 to 3.5; a  $s = 2$  value<sup>22b</sup> appears more reasonable since it smoothly reduces to the  $N^{-2}$  dependence of linear chains. For high molecular weight three-arm star hydrogenated polybutadienes in the melt ( $M_a/M_e \cong 6$ –25), the exponential dependence of the self-diffusivity on the molecular weight was confirmed,<sup>28</sup> but it so overwhelmed the behavior that the preexponential power dependence was impossible to establish with confidence. A similar exponential dependence was also observed for tracer diffusion of three-arm polystyrene stars in high molecular weight matrices.<sup>29,30a</sup> However, the exponential slowing down of the diffusivities was not observed in solution studies<sup>25–27</sup> on systems with  $N_a/N_e(\phi)$  up to about 2. Actually, the data showed that the difference in the diffusivities in solution between linear and three-arm polystyrenes or polybutadienes of the same total molecular weight was not significant,<sup>26</sup> with the two architectures maintaining essentially identical behavior beyond the semidilute regime; thus, reptation with its expected profound differences between linear and star molecules must indeed be confined to much higher  $N_a/N_e(\phi)$  values.

The expected dependence of diffusivities on coil size ( $g$  factor, eq 1) was not evident between linear and three-arm stars, either.  $g$  may be calculated as  $g = (3f_s - 2)/f_s^2$  with  $f_s$  being the functionality of the star;  $f_s = 3$  for a three-arm star and  $g$  is estimated as 0.78, i.e., not very different from 1 for its effect to be detectable within experimental uncertainty. The diffusivity data on 18-arm star polyisoprene solutions<sup>27</sup> of various molecular weights collapse nicely onto a master curve when plotted in the representation  $D/D_0$  vs  $cM^{-1}D_0^{-3}$  (Figure 4 in ref 27) with  $D_0$  the extrapolated trace diffusion at zero concentration,  $M$  the molecular weight, and  $c$  the

concentration; however, the superimposed data are consistently lower than those for linear homopolymers in solution when plotted in the same manner. Since the overlap concentration  $c^* \propto MR_g^{-3}$  and  $D_0 \propto R_h^{-1}$ , where  $R_h$  is the hydrodynamic radius (usually,  $R_h \propto R_g$ ), the above representation corresponds to the  $D/D_0$  vs  $dc^*$  used for semidilute solutions of linear chains<sup>32</sup> and does not take into consideration the size reduction discussed above. Besides, it was reported there that a shift of the star data along the  $x$ -axis by 2.5 results in a perfect superposition with the data for the linear homopolymers (for an 18-arm star,  $g = 0.16$  and its effect should be clearly detectable; for those stars, this factor 2.5 is equal to  $g^{-0.5}$ ). A different reduction procedure will be proposed in section 4 of the present paper. Moreover, the self-diffusion coefficients in polybutadiene three-arm star solutions were consistently lower<sup>26</sup> than the ones for polystyrene stars and showed a steeper concentration dependence, consistent with polybutadiene solutions approaching entangled behavior at lower concentrations than those of polystyrene because the  $N_e$  of polybutadiene is much lower than the  $N_e$  of polystyrene.

### 3. Experimental Section

**Materials.** A series of (polyisoprene)<sub>2</sub>(polystyrene), I<sub>2</sub>S, 3-miktoarm star copolymers (simple grafts) were synthesized by anionic polymerization using a high-vacuum technique in glass reactors provided with breakseals for the addition of reagents and constrictions for removal of products; the chlorosilane chemistry approach was utilized. Details on the synthesis and characterization on these systems have been described earlier.<sup>36,37</sup> Following standard purification of the monomers, the solvent, and the methyltrichlorosilane linking agent, the living polystyrenyllithium (PSLi) and polyisoprenyllithium (PILi) living arms were synthesized in benzene solution using *sec*-butyllithium as the initiator. For the  $\tau = 0.5$  I<sub>2</sub>S samples (Figure 1), the next step involved the reaction of a solution  $\sim 3\%$  w/v of PSLi in benzene with an excess (SiCl/Li = 100) of methyltrichlorosilane (CH<sub>3</sub>SiCl<sub>3</sub>) followed by a removal of the unreacted linking agent; next, an excess of PILi was added to a solution of the macromolecular difunctional linking agent, PS-Si(CH<sub>3</sub>)Cl<sub>2</sub>, to obtain the CH<sub>3</sub>Si(PS)(PI)<sub>2</sub> 3-miktoarm star copolymers I<sub>2</sub>S. The excess PILi was deactivated with degassed methanol. For the  $\tau = 0.25$  a-I<sub>2</sub>S samples (Figure 1), the procedure involved three steps, i.e., the reaction of the one isoprene arm (PI<sub>1</sub>Li) with an excess of CH<sub>3</sub>SiCl<sub>3</sub> and then removal of the excess, dropwise addition of the PSLi to the PI<sub>1</sub>-Si(CH<sub>3</sub>)Cl<sub>2</sub> solution and monitoring of the progress of the reaction, and then addition of an excess of the second polyisoprene arm (PI<sub>2</sub>Li) to the (PI<sub>1</sub>)(PS)(CH<sub>3</sub>)SiCl to obtain the CH<sub>3</sub>Si(PI<sub>1</sub>)(PS)(PI<sub>2</sub>) 3-miktoarm star copolymers a-I<sub>2</sub>S. The excess PILi was also deactivated with degassed methanol. In both cases, fractionation of the samples was performed by addition of methanol to a 1% solution of the polymers in a 60/40 benzene/hexane mixture; usually three fractionations were enough to remove any unlinked polyisoprene arms as monitored by size exclusion chromatography. The molecular characteristics of the samples obtained by membrane osmometry ( $M_n$ ), low-angle laser light scattering ( $M_w$ ), size exclusion chromatography SEC (polydispersity), and UV analysis (styrene content) are shown in Table 1. The microstructure of the dienic sequences was analyzed by <sup>1</sup>H- and <sup>13</sup>C-NMR spectroscopy to be ca. 90% 1,4 and ca. 10% 3,4. Note that in both the I<sub>2</sub>S and the a-I<sub>2</sub>S samples the polystyrene sequence is perdeuterated (styrene-*d*<sub>8</sub>), except for the higher molecular weight I<sub>2</sub>S-8. In Table 1 and in the following,  $f$  denotes the volume fraction of polyisoprene, which constitutes the backbone of the graft copolymer.

The polystyrene-polyisoprene diblocks, JG, to be used as reference materials were synthesized under high vacuum in a glass-sealed apparatus at room temperature using benzene as the solvent and *s*-BuLi as the initiator with styrene being polymerized first. After the completion of the reaction for both blocks, the living ends were neutralized with degassed methanol.

**Table 1. Molecular Characteristics of the (Polyisoprene)<sub>2</sub>(Polystyrene) Graft Copolymers**

species	$M_n$	$M_w$	$M_w/M_n$	$w_{PS}^a$	$N^b$	$f = f_{PI}^c$	$\tau^d$	$g^e$	$N_e^f$	$\phi_e^g$
I <sub>2</sub> S-1	97 100	106 000	1.04	0.91	1191	0.10	0.50	0.986	136.7	0.191
I <sub>2</sub> S-2	89 400	90 800	1.04	0.84	1031	0.18	0.50	0.960	127.3	0.206
I <sub>2</sub> S-3	83 000	87 400	1.04	0.67	1017	0.36	0.50	0.875	109.4	0.199
I <sub>2</sub> S-4	82 500	92 000	1.04	0.49	1098	0.54	0.50	0.799	95.1	0.181
I <sub>2</sub> S-5	82 600	89 800	1.04	0.35	1093	0.68	0.50	0.778	85.8	0.170
I <sub>2</sub> S-6	92 300	101 000	1.04	0.20	1254	0.82	0.50	0.818	77.7	0.137
I <sub>2</sub> S-7	84 300	91 300	1.06	0.10	1149	0.91	0.50	0.888	73.2	0.131
I <sub>2</sub> S-8	145 700	147 100	1.03	0.57 <sup>h</sup>	1716	0.48	0.50	0.820	99.5	0.129
a-I <sub>2</sub> S-1	97 500	101 400	1.04	0.33	1237	0.70	0.25	0.835	84.5	0.146
a-I <sub>2</sub> S-2	96 600	100 500	1.04	0.50	1198	0.54	0.25	0.849	95.1	0.161
a-I <sub>2</sub> S-3	95 700	99 500	1.04	0.67	1158	0.36	0.25	0.907	109.4	0.175

<sup>a</sup> Polystyrene weight fraction by SEC-UV. <sup>b</sup> Based on average segmental volume. <sup>c</sup> Polyisoprene volume fraction. <sup>d</sup> Position of the polystyrene graft along the polyisoprene chain. <sup>e</sup>  $g = 1 - 6f^2(1 - f\tau(1 - \tau))$ . <sup>f</sup>  $(N_e)_{diblock} = (fN_{e,A}^{-1/2} + (1 - f)N_{e,B}^{-1/2})^{-2}$ . <sup>g</sup>  $\phi_e = \{N_e/(gN)\}^{0.77}$ . <sup>h</sup> By <sup>1</sup>H-NMR in CDCl<sub>3</sub>.

**Table 2. Molecular Characteristics of the Linear Polystyrene–Polyisoprene Diblock Copolymers**

species	$M_n$	$M_w$	$M_w/M_n$	$w_{PS}^a$	$N^b$	$f = f_{PI}^c$	$N_e^d$	$\phi_e^e$
JG-1	89 000	96 000	1.08	0.62	1127	0.41	105	0.160
JG-2	130 000	140 500	1.08	0.41	1694	0.62	89	0.104
JG-3	84 000	89 000	1.06	0.43	1071	0.60	91	0.149
JG-4	54 700	57 500	1.05	0.56	679	0.47	100	0.229

<sup>a</sup> Polystyrene weight fraction by SEC-UV. <sup>b</sup> Based on average segmental volume. <sup>c</sup> Polyisoprene volume fraction. <sup>d</sup>  $(N_e)_{diblock} = (fN_{e,A}^{-1/2} + (1 - f)N_{e,B}^{-1/2})^{-2}$ . <sup>e</sup>  $\phi_e = (N_e/N)^{0.77}$ .

nol. Their molecular characteristics obtained as before are given in Table 2.

**Pulsed-Field-Gradient Nuclear Magnetic Resonance (PFG-NMR).** The basis of the technique is a stimulated echo measurement using the proton spin as a probe; it measures the mean-squared displacements  $\langle r^2 \rangle$  of particles bearing <sup>1</sup>H nuclei in a given time  $t$ , if two magnetic field gradients are applied as pulses during the spin echo experiment.<sup>38</sup> The field gradients with amplitude  $g$  and width  $\delta$  are separated by the time  $t$ , the diffusion time. If the motion of the particles is simple Fickian diffusion, then  $\langle r^2 \rangle = 6Dt$  and the translational self-diffusion coefficient  $D$  is obtained in the experiment. Deuterated toluene is used as the solvent for the copolymer solutions; thus, the diffusion of only the macromolecules is observed. The measured quantity is the attenuation of the spin echo  $\Psi$  due to diffusion if the field gradients are switched on. This echo attenuation may be written as a single particle correlation function

$$\Psi(q, t) \propto S_{inc}(q, t) \exp(-2\tau/T_2) \exp(-t/T_1) \quad (2)$$

$q = \gamma g \delta$  is the generalized wave vector<sup>39</sup> with  $\gamma$  being the gyromagnetic ratio of the proton. In eq 2, the last two terms describe the nuclear magnetic relaxation which also takes place in the experiments; however, in one experiment,  $\tau$  and  $t$  are fixed and these terms need not be considered.  $\tau$  is the time between the first two  $\pi/2$  - RF pulses, whereas  $T_1$  and  $T_2$  are the longitudinal and transverse relaxation times, respectively. We always use the "narrow pulse approximation", i.e.,  $\delta \ll t$  and  $\tau \ll t$ . The generalized wave vector may be varied via either the gradient amplitude  $g$  or the pulse duration  $\delta$ . However, switching the gradient on and off does not permit one to reduce  $\delta$  below about  $10^{-3}$  s. Moreover, large  $q$  values require strong magnetic field gradients and are limited by thermal and mechanical problems with the large currents in the field gradient coil. The range of  $q$  in the present experiments extends to about  $1.0 \times 10^{-3} \text{ \AA}^{-1}$ .  $S_{inc}(q, t)$  is the Fourier transform of the autocorrelation function for the proton position which may be identified with the normalized intermediate scattering function measured by incoherent neutron scattering. The longest accessible diffusion times are determined (eq 2) by the spin-lattice relaxation time  $T_1$  on the order of seconds;  $t$  may be varied between  $10^{-3}$  s and  $T_1$ . Measurements were performed for various diffusion times in the range of 30 to 300 ms; the data for the echo amplitude superimpose when plotted vs  $q^2 t$ , and this indicates normal diffusion with mean-squared displacement  $\langle r^2 \rangle \propto t$ .

The echo attenuations,  $S_{inc}(q, t)$ , were always to a very good approximation well represented by a single exponential decay function yielding the chain diffusivity  $D$  indicating a very low mass distribution in the samples:

$$S_{inc}(q, t) = a \exp[-q^2 D t] \quad (3)$$

Due to the presence of traces of protonated solvent molecules or residues of low molecular weight substances in the samples,  $a$  was in most cases slightly smaller but very near unity in the fits. In the samples I<sub>2</sub>S-2 and I<sub>2</sub>S-1, another faster process was indicated in the echo attenuations;  $S_{inc}(q, t)$  had to be analyzed with two exponentials where the slow one is assigned to the self-diffusion of the star molecule and the faster to the protonated low molecular weight substance probably present. Note that, in PFG-NMR, the part of the molecules in the NMR signal which have a self-diffusion coefficient  $D$  is proportional to the mass fraction of these molecules in the sample<sup>40</sup> and that low molecular weight tracers are generally more strongly weighted in the NMR signal due to their longer NMR relaxation times (cf. eq 2) in comparison with those of the polymer molecules.

#### 4. Results and Discussion

Figure 2a shows the echo amplitude  $S_{inc}(q, t)$  for a series of solutions in deuterated toluene of the I<sub>2</sub>S-7 graft rich in isoprene ( $f_{PI} = 0.91$ ) as a function of copolymer concentration; the concentrations examined place the solutions not only in the semidilute but also in the concentrated regime. The echo amplitudes are well represented by single exponential decay functions for all concentrations, as shown in Figure 2b, yielding the chain self-diffusion coefficients,  $D$ . The dependence of  $D$  on concentration, evident in Figure 2a, will be discussed later. With the exception of the I<sub>2</sub>S-2 and to a lesser extent the I<sub>2</sub>S-1 samples, where a second faster process is observed in  $S_{inc}(q, t)$  as noted in the Experimental Section above, all the other I<sub>2</sub>S and the three a-I<sub>2</sub>S samples show a very similar single exponential behavior. Due to the probable presence of lighter species at trace concentrations (e.g., traces of protonated solvent in the deuterated toluene used), the value of the amplitude  $a$  of  $S_{inc}(q, t)$ , eq 3, is slightly smaller than one in most cases.

Table 3 summarizes the self-diffusion data for both the I<sub>2</sub>S and the a-I<sub>2</sub>S grafts vs concentration in deuterated toluene, whereas Figure 3a shows the concentration dependence of the translational diffusivities in the solution for the I<sub>2</sub>S graft copolymers in a log-log representation. Two important characteristics are evident: the diffusivities do not show a simple power law dependence on concentration, and the data for the various grafts investigated do not overlap; the first observation is in agreement with similar observations for both homopolymer and diblock copolymer solutions

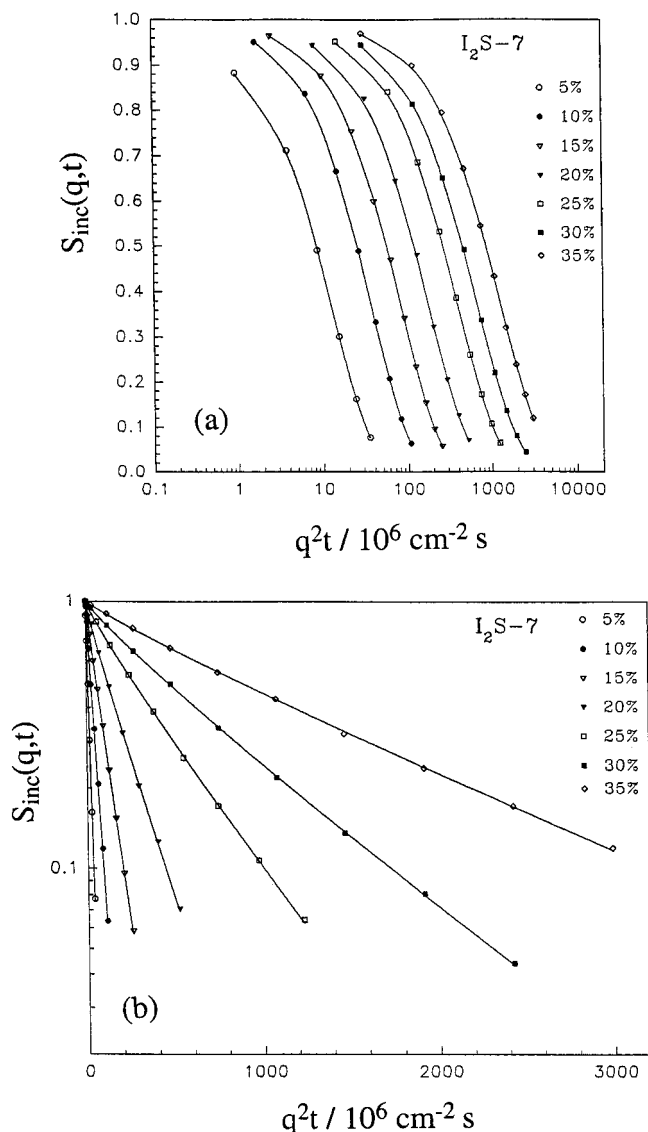


**Figure 2.** Spin-echo amplitude,  $S_{inc}(q,t)$ , for  $I_2S$ -7/toluene solutions at 25 °C for various concentrations as measured with PFG-NMR vs the product of the square of the effective scattering vector,  $q$ , and the time,  $t$ . The data for all concentrations are well represented by single exponential decay functions (b).

whereas the second agrees with the behavior of linear diblocks.<sup>18,19</sup> Similar characteristics are exhibited by the data for the a- $I_2S$  series depicted in Figure 3b. Actually, in both cases and in qualitative agreement with the linear diblock copolymer data, the diffusion coefficients for the polyisoprene rich grafts are consistently lower than those for the copolymers rich in styrene when compared at the same concentration over almost the whole concentration range investigated. Once more, this observation is against intuition if one thinks in terms of the probable higher frictions of polystyrene solutions relative to polyisoprene ones due to the significantly different dynamic chain flexibilities of the two homopolymers. This effect is attributed to the different entanglement characteristics of the parent homopolymers, similar to the case of diblock copolymers,<sup>18,19</sup> and it will be shown that the data sufficiently superimpose almost over the whole concentration range when the axes are appropriately reduced.

In order to discuss the self-diffusion data for the  $I_2S$  and a- $I_2S$  grafts in the semidilute to concentrated solution regime and on the basis of discussion in Section 2, one should consider three different concentration

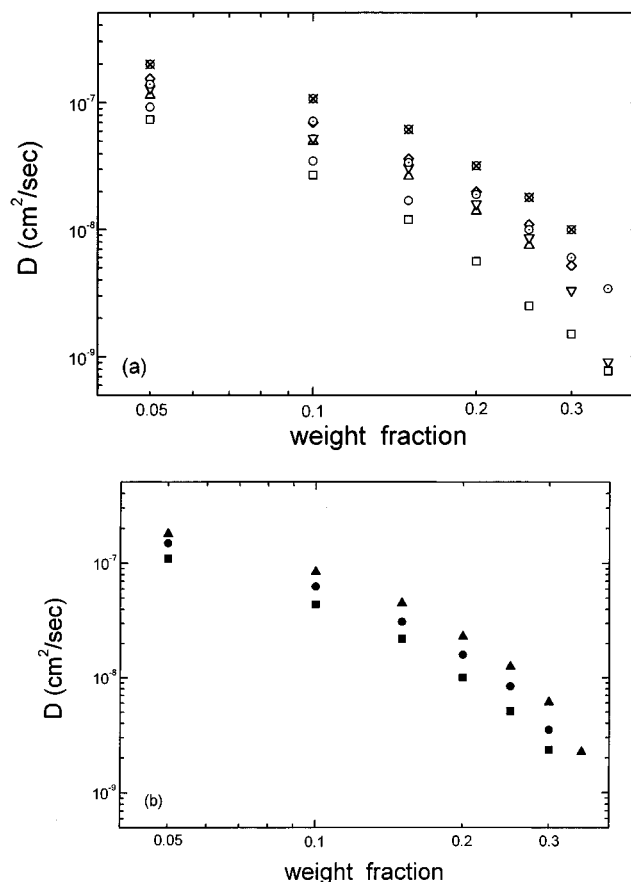


**Figure 3.** Concentration dependence of the self diffusion coefficients in the solution for (a) the  $I_2S$  and (b) the a- $I_2S$  graft copolymers in a log-log representation: (○)  $I_2S$ -1; (⊗)  $I_2S$ -2; (◇)  $I_2S$ -3; (▽)  $I_2S$ -4; (△)  $I_2S$ -5; (○)  $I_2S$ -6; (□)  $I_2S$ -7; (■) a- $I_2S$ -1; (●) a- $I_2S$ -2; (▲) a- $I_2S$ -3.

regimes: at low concentrations, the grafts should obey Rouse-Zimm dynamics with the possible difference from linear molecules attributed to their reduced size ( $g$  factor); at higher concentrations in the range of  $\phi_e$ , the transient behavior toward entanglement effects should become evident, similar to solutions of homopolymers and linear diblocks; at much higher concentrations, the systems should exhibit the star-like slowing down of the dynamics. These regimes depend on the molecular weight as well as on the entanglement molecular weights of the parent homopolymers. Since  $N_e(\phi) \cong N_e\phi^\beta$ ,  $\phi_e \cong (N_e/N)^{-1/\beta}$ , where in the rest the value  $\beta = 1/(1 - 3\nu) = -1.30$  with  $\nu = 0.59$  for good solvents will be used. On the basis of the discussion on the size reduction in section 2 above, the effective number of segments  $N_{eff} = gN$  will be used for the star molecules instead of  $N$ . The question of the effective  $N_e$  for a block copolymer surfaced in the work on diffusivities of linear diblocks,<sup>18,19</sup> where the mixing rule proposed for the plateau modulus of a homogeneous polymer blend<sup>41</sup> was adopted, leading to the expression  $N_e = (fN_{e,A})^{-1/2} + (1 - fN_{e,B})^{-1/2})^{-2}$  ( $N_{e,I}$  is the entanglement number of segments of homopolymer I); the number of entanglements per chain in solution are, then,  $n_e = N/N_e(\phi) = (N/N_e)\phi^{-\beta}$ . Alternatively, one may assume that the number of entanglements per a copolymer chain is simply the sum of the number of entanglements per each of the blocks  $n_e = [N_A/N_{e,A} + N_B/N_{e,B}]\phi^{-\beta} = N[fN_{e,A}^{-1} + (1 - fN_{e,B}^{-1})]\phi^{-\beta}$ . Effectively, the first equation assumes that the environment determines the number of entanglements whereas the second assumes that they are essentially determined by the reptating copolymer chain. For not extremely different values for

**Table 3. Self-Diffusion Coefficients of the (polyisoprene)<sub>2</sub>(polystyrene) Graft Copolymers in Toluene at 25 °C**

species	<i>D</i> [cm <sup>2</sup> /s]						
	5 wt %	10 wt %	15 wt %	20 wt %	25 wt %	30 wt %	35 wt %
I <sub>2</sub> S-1	1.4 × 10 <sup>-7</sup>	7.2 × 10 <sup>-8</sup>	3.4 × 10 <sup>-8</sup>	1.9 × 10 <sup>-8</sup>	1.0 × 10 <sup>-8</sup>	6.0 × 10 <sup>-9</sup>	3.4 × 10 <sup>-9</sup>
I <sub>2</sub> S-2	2.0 × 10 <sup>-7</sup>	1.1 × 10 <sup>-7</sup>	6.2 × 10 <sup>-8</sup>	3.2 × 10 <sup>-8</sup>	1.8 × 10 <sup>-8</sup>	1.0 × 10 <sup>-8</sup>	
I <sub>2</sub> S-3	1.6 × 10 <sup>-7</sup>	7.0 × 10 <sup>-8</sup>	3.7 × 10 <sup>-8</sup>	2.0 × 10 <sup>-8</sup>	1.1 × 10 <sup>-8</sup>	5.2 × 10 <sup>-9</sup>	
I <sub>2</sub> S-4	1.3 × 10 <sup>-7</sup>	5.3 × 10 <sup>-8</sup>	3.1 × 10 <sup>-8</sup>	1.6 × 10 <sup>-8</sup>	8.6 × 10 <sup>-9</sup>	3.3 × 10 <sup>-9</sup>	9.1 × 10 <sup>-10</sup>
I <sub>2</sub> S-5	1.2 × 10 <sup>-7</sup>	5.0 × 10 <sup>-8</sup>	2.7 × 10 <sup>-8</sup>	1.4 × 10 <sup>-8</sup>	7.5 × 10 <sup>-9</sup>		
I <sub>2</sub> S-6	9.3 × 10 <sup>-8</sup>	3.5 × 10 <sup>-8</sup>	1.7 × 10 <sup>-8</sup>				
I <sub>2</sub> S-7	7.4 × 10 <sup>-8</sup>	2.7 × 10 <sup>-8</sup>	1.2 × 10 <sup>-8</sup>	5.6 × 10 <sup>-9</sup>	2.5 × 10 <sup>-9</sup>	1.5 × 10 <sup>-9</sup>	7.7 × 10 <sup>-10</sup>
I <sub>2</sub> S-8	9.4 × 10 <sup>-8</sup>	4.1 × 10 <sup>-8</sup>	1.7 × 10 <sup>-8</sup>	6.9 × 10 <sup>-9</sup>	2.6 × 10 <sup>-9</sup>	8.1 × 10 <sup>-10</sup>	
a-I <sub>2</sub> S-1	1.1 × 10 <sup>-7</sup>	4.4 × 10 <sup>-8</sup>	2.2 × 10 <sup>-8</sup>	1.0 × 10 <sup>-8</sup>	5.1 × 10 <sup>-9</sup>	2.4 × 10 <sup>-9</sup>	
a-I <sub>2</sub> S-2	1.5 × 10 <sup>-7</sup>	6.3 × 10 <sup>-8</sup>	3.1 × 10 <sup>-8</sup>	1.6 × 10 <sup>-8</sup>	8.4 × 10 <sup>-9</sup>	3.5 × 10 <sup>-9</sup>	
a-I <sub>2</sub> S-3	1.8 × 10 <sup>-7</sup>	8.4 × 10 <sup>-8</sup>	4.5 × 10 <sup>-8</sup>	2.3 × 10 <sup>-8</sup>	1.3 × 10 <sup>-8</sup>	6.1 × 10 <sup>-9</sup>	2.3 × 10 <sup>-9</sup>

the two individual  $N_e$ 's, even in the case of polystyrene and polyisoprene investigated here, the two expressions give similar results; in the following the first formula is being used (Tables 1 and 2). It should be noted that the use of the above expressions for the branched molecules assumes that the molecular architecture does not influence the characteristic molecular weight for reptation.<sup>23a</sup>

Therefore, for low and moderate  $n_e$ 's, the behavior of the stars should be close to that of linear diblocks taking into account the factor  $g$  due to the different coil sizes;  $g = 1$  for linear polymers. Adaptation, then, of the predicted behavior for linear homopolymers in semidilute solutions to star molecules leads to the following expressions<sup>32,42</sup> for the self-diffusion coefficients in the Rouse and the entanglement regimes (low  $n_e$ 's):

$$D(N, \phi) \cong \frac{kT}{\eta_s b} \frac{1}{gN} \phi^{-(1-\nu)/(3\nu-1)} = \frac{kT}{\eta_s b} \frac{1}{gN} \phi^{-0.53} \quad [n_e \ll 1] \quad (4a)$$

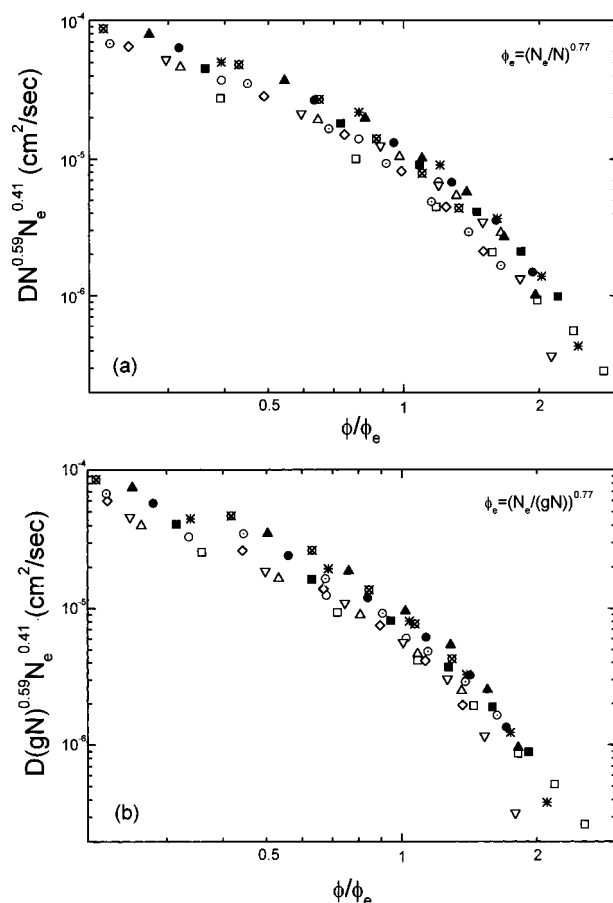
$$D(N, \phi) \cong \frac{kT}{\eta_s b} \frac{N_e}{(gN)^2} \phi^{-(2-\nu)/(3\nu-1)} = \frac{kT}{\eta_s b} \frac{N_e}{(gN)^2} \phi^{-1.83} \quad [n_e \cong O(1)] \quad (4b)$$

The behavior of linear diblocks qualitatively<sup>19</sup> follows the trend suggested by the above dependencies. Using the concentration  $\phi_e = \{N_e/(gN)\}^{3\nu-1}$ , the above equations become

$$D(N, \phi) \cong \frac{kT}{\eta_s b} (gN)^{-\nu} N_e^{-1+\nu} (\phi/\phi_e)^{-(1-\nu)/(3\nu-1)} = \frac{kT}{\eta_s b} (gN)^{-0.59} N_e^{-0.41} (\phi/\phi_e)^{-0.53} \quad (5a)$$

$$D(N, \phi) \cong \frac{kT}{\eta_s b} (gN)^{-\nu} N_e^{-1+\nu} (\phi/\phi_e)^{-(2-\nu)/(3\nu-1)} = \frac{kT}{\eta_s b} (gN)^{-0.59} N_e^{-0.41} (\phi/\phi_e)^{-1.83} \quad (5b)$$

Figure 4a shows the diffusion data for both the I<sub>2</sub>S and the a-I<sub>2</sub>S series plotted in a representation equivalent to eq 5a and 5b with  $\nu = 0.59$ , i.e.,  $[DN^{0.59}N_e^{0.41}]$  vs  $[\phi/\phi_e]$  and without taking into account the  $g$  size reduction (by setting  $g = 1$ ). It should be noted that, since the trace diffusion coefficient in good solvents  $D_0 \propto N^{-\nu} \cong N^{-0.59}$  and since  $\phi_e \propto N_e^{3\nu-1} c^* \cong N_e^{0.77} c^*$ , the above representation is equivalent to the extensively used  $D/D_0$  vs  $c/c^*$  scaling when comparing solutions of the same linear polymer (constant  $N_e$ ); for different  $N_e$ 's, however, the  $N_e$  factor should be taken into account.<sup>43,19</sup> The differences between the data for the various grafts

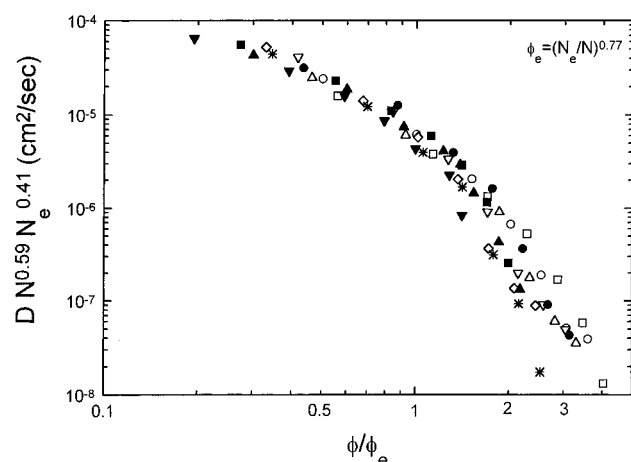


**Figure 4.** (a) Self-diffusion coefficients of the I<sub>2</sub>S and the a-I<sub>2</sub>S grafts in toluene solutions in a representation suggested by eqs 5a and 5b without taking into account the  $g$  coil size ratio reduction, i.e.,  $DN^{0.59}N_e^{0.41}$  as a function of the concentration  $\phi$  reduced to the concentration  $\phi_e = (N_e/N)^{0.77}$ , above which entanglement effects should become important. (b) Self-diffusion data in part a plotted as  $[D(gN)^{0.59}N_e^{0.41}]$  vs  $[\phi/\phi_e]$  with  $\phi_e = [N_e/(gN)]^{0.77}$ : (○) I<sub>2</sub>S-1; (⊗) I<sub>2</sub>S-2; (◇) I<sub>2</sub>S-3; (▽) I<sub>2</sub>S-4; (Δ) I<sub>2</sub>S-5; (○) I<sub>2</sub>S-6; (□) I<sub>2</sub>S-7; (\*) I<sub>2</sub>S-8; (■) a-I<sub>2</sub>S-1; (●) a-I<sub>2</sub>S-2; (▲) a-I<sub>2</sub>S-3.

of each series in Figure 4a is much reduced compared to parts a and b of Figure 3, indicating that such a reduced plot can account for the different entanglement characteristics of the samples (for those materials the  $D_0$  and  $c^*$  values are very similar due to the very similar molecular weights). In the same figure, the appropriately reduced data are included for the I<sub>2</sub>S-8 graft, which possesses a higher molecular weight than the rest of the I<sub>2</sub>S series; it is evident that the proposed scaling by the above equations can also account for the molecular weight effects. No single power law behavior is observed for the concentration dependence, with the data showing a progressive change of slope from the exponent of eq 5a to that of eq 5b and even higher; for

**Table 4.** Self-Diffusion Coefficients of the Linear Polystyrene–Polyisoprene Diblock Copolymers in Toluene at 25 °C

species	$D$ [cm <sup>2</sup> /s]						
	5 wt %	10 wt %	15 wt %	20 wt %	25 wt %	30 wt %	35 wt %
JG-1	$1.3 \times 10^{-7}$	$5.4 \times 10^{-8}$	$2.6 \times 10^{-8}$	$1.4 \times 10^{-8}$	$6.8 \times 10^{-9}$	$2.7 \times 10^{-9}$	$6.0 \times 10^{-10}$
JG-2	$6.2 \times 10^{-8}$	$2.5 \times 10^{-8}$	$7.8 \times 10^{-9}$	$3.2 \times 10^{-9}$	$7.2 \times 10^{-10}$	$1.8 \times 10^{-10}$	$8.5 \times 10^{-11}$
JG-3	$1.1 \times 10^{-7}$	$4.8 \times 10^{-8}$	$1.9 \times 10^{-8}$	$1.1 \times 10^{-8}$	$3.7 \times 10^{-9}$	$1.1 \times 10^{-9}$	$3.4 \times 10^{-10}$
JG-4	$2.1 \times 10^{-7}$	$9.5 \times 10^{-8}$	$5.1 \times 10^{-8}$	$2.8 \times 10^{-8}$	$1.4 \times 10^{-8}$	$7.3 \times 10^{-9}$	$2.7 \times 10^{-9}$

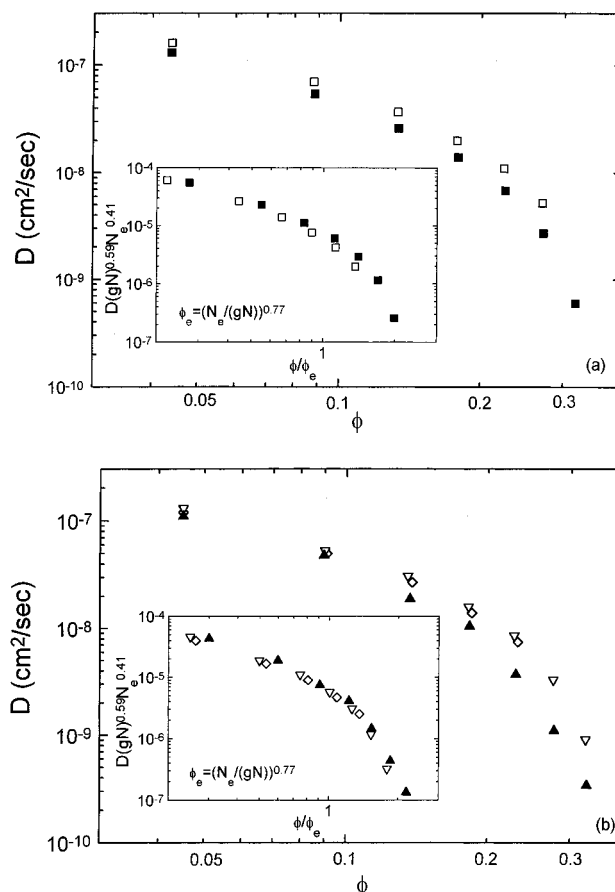
**Figure 5.** Self-diffusion coefficients of the SI<sup>19</sup> and JG diblock copolymers in toluene solutions in a representation suggested by eq 5a and 5b, i.e.,  $DN^{0.59}N_e^{0.41}$  as a function of the concentration  $\phi$  reduced to the concentration  $\phi_e = (N_e/N)^{0.77}$ , above which entanglement effects should become important; here  $g = 1$ : (□) SI-20; (○) SI-30; (△) SI-36; (▽) SI-57; (◇) SI-68; (\*) SI-76; (■) JG-1; (●) JG-2; (▲) JG-3; (▼) JG-4.

both homopolymer and linear diblock copolymer solutions<sup>19</sup> the data at higher concentrations approaching the concentrated solution regime showed an apparent  $(\phi/\phi_e)^3$  behavior (obtained from eq 5b for  $\nu \cong 0.5$  due to a progressive change to Gaussian behavior in concentrated solutions) followed by an even stronger dependence when the solution friction effects became important. Moreover, the data for the a-I<sub>2</sub>S samples ( $\tau = 0.25$ ) are apparently slightly higher than those for the I<sub>2</sub>S series ( $\tau = 0.50$ ). One may, thus, consider that the differences in the coil sizes of the various grafts have to be taken into account. The  $g$  factor for these graft block copolymers can be estimated using the following equation<sup>3,44</sup>

$$g = 1 - 6f^2(1 - f\tau(1 - \tau)) \quad (6)$$

where it is seen that both the composition  $f$  and the position of the graft  $\tau$  affect the coil size; the  $g$  values are shown in Table 1. Figure 4b shows the data of Figure 4a now plotted in the representation  $[D(gN)^{0.59}N_e^{0.41}]$  vs  $[\phi/\phi_e]$  with  $\phi_e = [N_e/(gN)]^{0.77}$ . The superposition between the I<sub>2</sub>S and the a-I<sub>2</sub>S data is not significantly improved due to the small variation in the  $g$  values.

At this stage, one should compare the diffusion data for the I<sub>2</sub>S and a-I<sub>2</sub>S simple grafts with data for linear diblock copolymers. In a previous investigation,<sup>19</sup> the diffusivities were measured by PFG-NMR on a series of polystyrene–polyisoprene diblock copolymers (SI series) in toluene solutions. Since the molecular weights of the old SI series were in the range of 150 000–160 000, measurements were performed on another series of polystyrene–polyisoprene diblocks with varying molecular weights, i.e., the JG series of Table 2. The single exponential behavior of the echo amplitude  $S_{inc}(q, t)$  as a function of  $q^2 t$  for various concentrations was once more verified as in the earlier investigation;<sup>19</sup> the

**Figure 6.** Comparison of the raw self-diffusion coefficients of simple graft and linear diblock copolymers of similar molecular weights and compositions vs concentration in toluene at 25 °C: (a) I<sub>2</sub>S-3 (□) vs JG-1 (■); (b) I<sub>2</sub>S-4 (▽) and I<sub>2</sub>S-5 (◇) vs JG-3 (▲). The insets show the data in the representation  $[D(gN)^{0.59}N_e^{0.41}]$  vs  $[\phi/\phi_e]$  with  $\phi_e = [N_e/(gN)]^{0.77}$ .

diffusion coefficients are listed in Table 4 for all the JG samples. In the previous investigation,<sup>19</sup> where the  $\phi/\phi_e$  scaling for diblock copolymer solutions was first introduced, the data were depicted as  $DN^2$  vs  $\phi/\phi_e$  with the  $\phi_e$  calculated using  $\delta = -1$ ; the  $N^2$  correction was introduced to account for the slight differences in the molecular weights among the old SI samples based on the scaling of eq 4b. In Figure 5, the data on the new JG series are shown together with the previously measured diffusion data on the linear SI series with the representation of Figure 4a, i.e.,  $[DN^{0.59}N_e^{0.41}]$  vs  $[\phi/\phi_e]$ , with  $\phi_e = [N_e/N]^{0.77}$ ; a much better superposition of the data is obtained than that shown in Figure 5 of ref 19. Moreover, this representation accounts very nicely for the combined effects of molecular weight and composition on the diffusivities of linear diblocks; when the diffusivities of an one million molecular weight symmetric diblock (SI-1M in ref 45) are similarly normalized (not shown), the diffusion coefficients (which were different by almost three orders of magnitude) conform within a factor of 3 to the data in Figure 5. The SI-1M diffusivities can be brought into an excellent agreement with the SI and JG series when the effective exponent

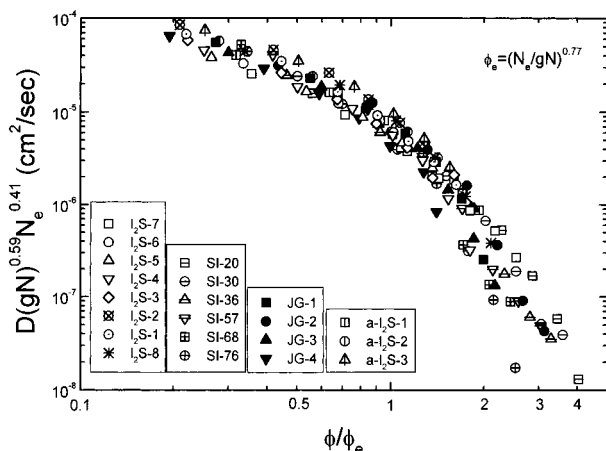


**Figure 7.** Self-diffusion coefficients of the I<sub>2</sub>S and the a-I<sub>2</sub>S grafts as well as of the SI<sup>19</sup> and JG linear diblocks in toluene solutions in the representation  $[D(gN)^{0.59}N_e^{0.41}]$  vs  $[\phi/\phi_e]$  with  $\phi_e = [N_e/(gN)]^{0.77}$ .

$\nu$  is modified to  $\nu \cong 0.55$ ; a  $D_0 \propto M^x$  dependence with  $x$  in the range  $-0.52$  to  $-0.6$  of the zero-concentration trace diffusivity on molecular weight has been observed before for various polymer/solvent systems as a function of solvent quality.<sup>24,32,33</sup> However, an attempt to optimize the exponent  $x$ , which would have given the best superposition, is not attempted, since the molecular weight range of the present study is not wide enough for an acceptable accuracy in the determination of  $x$  for diblock copolymers; this investigation will be undertaken in the future.

The raw self-diffusion data as a function of concentration are compared in Figure 6a between the I<sub>2</sub>S-3 graft and the JG-1 linear diblock; these two samples have almost the same molecular weight and very similar compositions (therefore, similar  $N_e$ 's and similar  $\phi_e$ 's) but differ in their architecture. A similar comparison is made in Figure 6b between I<sub>2</sub>S-4 and I<sub>2</sub>S-5 grafts and the JG-3 diblock; the samples have similar molecular weights and the linear has a composition right in between the two grafts. The diffusion for the linear diblocks in both cases is consistently slower than for the respective grafts although the differences are small (at the higher concentrations the difference is less than a factor of 3); this agrees with earlier findings<sup>22a,23a</sup> that the viscosities of star homopolymers are lower than those for their linear counterparts at low concentrations and that the differences between linear and three-arm stars are very small. As discussed earlier, this can be explained by the smaller size of the graft copolymer<sup>21</sup> and can be quantitatively accounted for when the data are plotted as  $[D(gN)^{0.59}N_e^{0.41}]$  vs  $[\phi/\phi_e]$  (as in Figure 4b), shown in the insets of parts a and b of Figure 6. Therefore, although the inclusion of the  $g$  size reduction does not apparently improve the data superposition in Figure 4b relative to Figure 4a, it is evident that its inclusion in the expressions for the self diffusivities in eq 4 and 5 appropriately corrects for the small but real differences in the behavior between linear and star block copolymers.

Finally, a comparison is attempted in Figure 7 between the data for the I<sub>2</sub>S and a-I<sub>2</sub>S grafts and the SI and JG linear diblocks using the representation of Figure 4b, i.e., as  $[D(gN)^{0.59}N_e^{0.41}]$  vs  $[\phi/\phi_e]$  with  $\phi_e = [N_e/(gN)]^{0.77}$ . The data for such an extended series of samples collapse quite satisfactory onto a master curve over the whole concentration range. Note, however, that once more the data in this figure do not conform to the exponents predicted for the concentration depen-

dence by eq 5a and 5b; i.e., there are no concentration regimes exhibiting clear power law dependencies.

The exponential slowing down of the diffusivities expected for well-entangled star molecules is not observed in any of the systems investigated here. This is in accordance with the earlier observation<sup>22a,23a</sup> that viscosity enhancement can only be observed when the parameter  $\Omega = Z\phi^{5/6}(\phi M_a/2M_c)$  is significantly higher than 1;  $Z$  is a polymer specific constant ( $0.078 \text{ \AA}^{-1}$  for polystyrene and  $0.103 \text{ \AA}^{-1}$  for polyisoprene), and  $M_c$  is the critical molecular weight for entanglement in the bulk ( $M_c \cong 2M_e$ ). For the solutions investigated in this work, the value of the  $\Omega$  parameter is in the range of 0.35, and therefore, no enhancement should be observed according to Figure 7 of ref 22a.

## 5. Concluding Remarks

The composition and concentration dependence of the self-diffusion coefficients of a series of simple graft copolymers of polystyrene grafts on a polyisoprene backbone has been investigated in solutions in the neutral good solvent toluene by pulsed-field-gradient nuclear magnetic resonance. Two kinds of architectures were investigated: one series with the graft situated at the middle of the isoprene block and one with the graft at a 25:75 position. The observed composition and architecture dependence of the diffusivities can be quantitatively accounted for and the data for both the graft- and the diblock-copolymers collapse nicely onto a master curve when plotted as  $[D(gN)^{0.59}N_e^{0.41}]$  vs  $[\phi/\phi_e]$  with  $\phi_e = [N_e/(gN)]^{0.77}$ ; i.e., when the differences in the entanglement characteristics of the parent homopolymers (via  $N_e$ ) and the different radii of gyration of stars vs linear polymers (via  $g$ ) are taken into account. The exponential slowing down of the diffusivities expected for star molecules was not observed due to low entanglement densities in all our systems. Moreover, the concentration dependence of the self-diffusion coefficients for graft copolymers showed a behavior similar to that for homopolymer and linear diblock copolymer solutions, i.e., a continuous decrease of the diffusivities when the concentration increases without a clear power law exponent over significant concentration regimes.

The same series of graft copolymers is currently being investigated<sup>46</sup> with dynamic light scattering in order to evaluate the mechanisms of relaxation of concentration fluctuations in solutions; one aim is to establish whether the polydispersity diffusive relaxation observed in linear diblock copolymer solutions and identified with the self-diffusivity of the copolymer chains behaves similarly for the simple graft copolymers case. Besides, the behavior of the internal copolymer relaxation in these systems will provide information on their viscoelastic properties. The effect of copolymer architecture is also under investigation utilizing A-B-A-B linear tetrablocks and inverse starblock copolymers.

**Acknowledgment.** We are grateful to Prof. A. N. Semenov and Dr. I. Nyrkova for stimulating discussions and critical reading of the manuscript as well as to Dr. J. E. L. Roovers for very useful discussions. S.H.A. would like to acknowledge that part of this research was sponsored by NATO's Scientific Affairs Division in the framework of the Science for Stability Programme and by the Greek General Secretariat of Research and Technology. G.F. acknowledges financial support from the Deutsche Forschungsgemeinschaft (SFB 294). J.W.M., S.P., and M.P. acknowledge funding from the U.S. Army Research Office under Contract DAAH04-94-G-0245.



## References and Notes

- (1) Bates, F. S.; Fredrickson, G. H. *Annu. Rev. Phys. Chem.* **1990**, *41*, 525. Bates, F. S. *Science* **1991**, *251*, 898. *Thermoplastic Elastomers—A Comprehensive Review*; Legge, R., Holden, N. R., Schroeder, H. E., Eds.; Hanser Publishers: Munich, 1988.
- (2) Leibler, L. *Macromolecules* **1980**, *13*, 1602. Fredrickson, G. H.; Helfand, E. *J. Chem. Phys.* **1987**, *87*, 697. Barrat, G. L.; Fredrickson, G. H. *J. Chem. Phys.* **1991**, *95*, 1282.
- (3) Olvera de la Cruz, M.; Sanchez, I. C. *Macromolecules* **1986**, *19*, 2501.
- (4) Benoit, H.; Hadziioannou, G. *Macromolecules* **1988**, *21*, 1449. Mayes, A. M.; Olvera de la Cruz, M. *J. Chem. Phys.* **1989**, *91*, 7228. Mayes, A. M.; Olvera de la Cruz, M. *J. Chem. Phys.* **1991**, *95*, 4670. Dobrynin, A. V.; Erukhimovich, I. Ya. *J. Phys. 2 (Fr.)* **1991**, *1*, 1387. Dobrynin, A. V.; Erukhimovich, I. Ya. *Macromolecules* **1993**, *26*, 276. Shinozaki, A.; Jasnow, G.; Balazs, A. C. *Macromolecules* **1994**, *27*, 2496.
- (5) Koberstein, J. T.; Russell, T. P.; Walsh, D. J.; Pottick, L. *Macromolecules* **1990**, *23*, 877. Gehlsen, M. D.; Almdal, K.; Bates, F. S. *Macromolecules* **1992**, *25*, 939. Floudas, G.; Hadjichristidis, N.; Iatrou, H.; Pakula, T.; Fischer, E. W. *Macromolecules* **1994**, *27*, 7735.
- (6) Hashimoto, T.; Shibayama, M.; Kawai, H. *Macromolecules* **1983**, *16*, 1093. Shibayama, M.; Hashimoto, T.; Hasegawa, H.; Kawai, H. *Macromolecules* **1983**, *16*, 1427. Hashimoto, T.; Kowasaka, K.; Shibayama, M.; Kawai, H. *Macromolecules* **1986**, *19*, 754. Hashimoto, T.; Mori, K. *Macromolecules* **1990**, *23*, 5347. Lodge, T. P.; Pan, C.; Jin, X.; Liu, Z.; Zhao, J.; Maurer, W. W.; Bates, F. S. *J. Polym. Sci.: Part B: Polym. Phys.* **1995**, *33*, 2289.
- (7) Benmouna, M.; Benoit, H. *J. Polym. Sci., Polym. Phys. Ed.* **1983**, *21*, 1227. Benoit, H.; Wu, W.; Benmouna, M.; Mozer, B.; Bauer, B.; Lapp, A. *Macromolecules* **1985**, *18*, 986. Hong, K. M.; Noolandi, J. *Macromolecules* **1983**, *16*, 1083. Onuki, A.; Hashimoto, T. *Macromolecules* **1989**, *22*, 879. Olvera de la Cruz, M. *J. Chem. Phys.* **1989**, *90*, 1995. Fredrickson, G. H.; Leibler, L. *Macromolecules* **1989**, *22*, 1238.
- (8) Fytas, G.; Anastasiadis, S. H. In *Disorder Effects on Relaxation Processes*; Richert, R., Blumen, A., Eds.; Springer Verlag: Berlin, 1994, and references therein.
- (9) Fredrickson, G. H.; Bates, F. S. *Annu. Rev. Phys. Chem.* **1996**, *26*, 501 and references therein.
- (10) Shull, K. R.; Kramer, E. J.; Bates, F. S.; Rosedale, J. H. *Macromolecules* **1991**, *24*, 1383. Dalvi, M. C.; Lodge, T. P. *Macromolecules* **1993**, *26*, 859. Dalvi, M. C.; Eastman, C. E.; Lodge, T. P. *Phys. Rev. Lett.* **1993**, *71*, 2591. Dalvi, M. C.; Lodge, T. P. *Macromolecules* **1994**, *27*, 3487. Leibig, C. M.; Fredrickson, G. H. *J. Polym. Sci.: Part B: Polym. Phys.* **1996**, *34*, 163.
- (11) Ehlich, D.; Takenaka, M.; Okamoto, S.; Hashimoto, T. *Macromolecules* **1993**, *26*, 189. Ehlich, D.; Takenaka, M.; Hashimoto, T. *Macromolecules* **1993**, *26*, 492.
- (12) Fleischer, G.; Fujara, F.; Stühn, B. *Macromolecules* **1993**, *26*, 2340.
- (13) Vogt, S.; Anastasiadis, S. H.; Fytas, G.; Fischer, E. W. *Macromolecules* **1994**, *27*, 4335.
- (14) Inoue, T.; Kishine, M.; Nemoto, N.; Kurata, M. *Macromolecules* **1989**, *22*, 496.
- (15) Balsara, N. P.; Stepanek, P.; Lodge, T. P.; Tirrell, M. *Macromolecules* **1991**, *24*, 6227. Balsara, N. P.; Eastman, C. E.; Foster, M. D.; Lodge, T. P.; Tirrell, M. *Makromol. Chem., Macromol. Symp.* **1991**, *45*, 213.
- (16) Jian, T.; Anastasiadis, S. H.; Semenov, A. N.; Fytas, G.; Adachi, K.; Kotaka, T. *Macromolecules* **1994**, *27*, 4762.
- (17) Lodge, T. P.; Dalvi, M. C. *Phys. Rev. Lett.* **1995**, *75*, 657.
- (18) Jian, T.; Anastasiadis, S. H.; Fytas, G.; Fleischer, G.; Vilesov, A. D. *Macromolecules* **1995**, *28*, 2439.
- (19) Anastasiadis, S. H.; Chrissopoulou, K.; Fytas, G.; Appel, M.; Fleischer, G.; Adachi, K.; Gallot, Y. *Acta Polym.* **1996**, *47*, 250.
- (20) de Gennes, P.-G. *J. Phys. (Les Ulis, Fr.)* **1975**, *36*, 1199.
- (21) Ham, J. S. *J. Chem. Phys.* **1957**, *26*, 625. Bueche, F. *J. Chem. Phys.* **1964**, *40*, 484. Berry, G. C.; Fox, T. G. *Adv. Polym. Sci.* **1968**, *5*, 261.
- (22) Graessley, W. W. *Acc. Chem. Res.* **1977**, *10*, 332. Graessley, W. W. *Adv. Polym. Sci.* **1982**, *47*, 67. Graessley, W. W. In *Physical Properties of Polymers*, 2nd ed.; ACS Professional Reference Book; American Chemical Society: Washington, DC, 1993; p 97.
- (23) Graessley, W. W.; Masuda, T.; Roovers, J. E. L.; Hadjichristidis, N. *Macromolecules* **1976**, *9*, 127. Pearson, D. S.; Mueller, S. J.; Fetters, L. J.; Hadjichristidis, N. *J. Polym. Sci., Polym. Phys. Ed.* **1983**, *21*, 2287. Hadjichristidis, N.; Roovers, J. *Polymer* **1985**, *26*, 1087. Roovers, J. *Polymer* **1985**, *26*, 1091. Carella, J. M.; Gotro, J. T.; Graessley, W. W. *Macromolecules* **1986**, *19*, 659. Masuda, T.; Ohta, Y.; Onogi, S. In *Current Topics in Polymer Science*; Ottenbrite, S., Utracki, L. A., Inoue, T., Eds.; Hanser: New York, 1987; Vol. II, p 109. Roovers, J.; Toporowski, P.; Martin, J. *Macromolecules* **1989**, *22*, 1897. Fetters, L. J.; Kiss, A. D.; Pearson, D. S.; Quack, G. F.; Vitus, F. J. *Macromolecules* **1993**, *26*, 647.
- (24) Kuzuu, N. Y. *J. Polym. Sci., Polym. Lett.* **1980**, *18*, 775. Pearson, D. S.; Raju, V. R. *Macromolecules* **1982**, *15*, 294. Needs, R. J.; Edwards, S. F. *Macromolecules* **1983**, *16*, 1492. Pearson, D. S.; Helfand, E. *Macromolecules* **1984**, *17*, 888. Marrucci, G. In *Advances in Transport Processes*; Mujumdar, A. S.; Mashelkar, R. A., Eds.; Wiley: New York, 1984, Vol. V. Klein, J. *Macromolecules* **1986**, *19*, 105. Rubinstein, M. *Phys. Rev. Lett.* **1986**, *57*, 3023. Grest, G. S.; Kremer, K.; Milner, S. T.; Witten, T. A. *Macromolecules* **1989**, *22*, 1904. Ball, R. C.; McLeish, T. C. B. *Macromolecules* **1989**, *22*, 1911. Brochard-Wyart, F.; Ajdari, A.; Leibler, L.; Rubinstein, M.; Viovy, J. L. *Macromolecules* **1994**, *27*, 803. McLeish, T. C. B.; Semenov, A. N. *Macromolecules* **1994**, *27*, 7205.
- (25) von Meerwall, E.; Tomich, D. H.; Hadjichristidis, N.; Fetters, L. J. *Macromolecules* **1982**, *15*, 1157.
- (26) von Meerwall, E.; Tomich, D. H.; Grisby, J.; Pennisi, R. W.; Fetters, L. J.; Hadjichristidis, N. *Macromolecules* **1983**, *16*, 1715.
- (27) Xuexin, C.; Zhongde, X.; von Meerwall, E.; Seung, N.; Hadjichristidis, N.; Fetters, L. J. *Macromolecules* **1984**, *17*, 1343.
- (28) Bartels, C. R.; Crist, B., Jr.; Fetters, L. J.; Hadjichristidis, N. *Macromolecules* **1986**, *19*, 785.
- (29) Antonietti, M.; Sillescu, H. *Macromolecules* **1986**, *19*, 798.
- (30) Shull, K. R.; Kramer, E. J.; Fetters, L. J. *Nature* **1990**, *345*, 790. Shull, K. R.; Dai, K. H.; Kramer, E. J.; Fetters, L. J.; Antonietti, M.; Sillescu, H. *Macromolecules* **1991**, *24*, 505.
- (31) Graessley, W. W.; Edwards, S. F. *Polymer* **1981**, *22*, 1329.
- (32) de Gennes, P. G. *Scaling Concepts in Polymer Physics*; Cornell University Press: Ithaca, NY, 1979. Doi, M.; Edwards, S. F. *The Theory of Polymer Dynamics*; Oxford Science Publishers: Oxford, England, 1986.
- (33) Douglas, J. F.; Hubbard, J. B. *Macromolecules* **1991**, *24*, 3163.
- (34) Schweizer, K. S.; Szamel, G. *Macromolecules* **1995**, *28*, 7543.
- (35) Roovers, J.; Graessley, W. W. *Macromolecules* **1981**, *14*, 766.
- (36) Pochan, D. J.; Gido, S. P.; Pispas, S.; Mays, J. W.; Ryan, A. J.; Fairclough, J. P. A.; Hamley, I. W.; Terrill, N. J. *Macromolecules* **1996**, *29*, 5091. Pochan, D. J.; Gido, S. P.; Pispas, S.; Mays, J. W. *Macromolecules* **1996**, *29*, 5099.
- (37) Iatrou, H.; Hadjichristidis, N. *Macromolecules* **1992**, *25*, 4649. Iatrou, H.; Siakali-Kioulafa, E.; Hadjichristidis, N.; Roovers, J.; Mays, J. W. *J. Polym. Sci., Part B: Polym. Phys. Ed.* **1995**, *33*, 1925.
- (38) Kärger, J.; Pfeifer, H.; Heink, W. *Adv. Magn. Reson.* **1988**, *12*, 1.
- (39) Fleischer, G.; Fujara, F. *NMR as a Generalized Scattering Experiment*. In *NMR-Basic Principles and Progress*; Kosfeld, R., Blümich, B., Eds.; Springer Verlag: Berlin, 1994; Vol. 30, p. 159. Kärger, J.; Fleischer, G. *Trends Anal. Chem.* **1994**, *13*, 145.
- (40) Fleischer, G.; Zgadzai, O. E.; Skirda, V. D.; Maklakov, A. I. *Colloid Polym. Sci.* **1988**, *266*, 201. Fleischer, G.; Zgadzai, O. E. *Colloid Polym. Sci.* **1988**, *266*, 208.
- (41) Tsenoglou, C. *J. Polym. Sci., Polym. Phys. Ed.* **1988**, *26*, 2329. Composto, R. J.; Kramer, E. J.; White, D. M. *Macromolecules* **1992**, *25*, 4167.
- (42) In eq 1a of ref 19, the factor  $N_e$  in the numerator of eq 4b was missing.
- (43) Raspaut, E.; Lairez, D.; Adam, M. *Macromolecules* **1995**, *28*, 927.
- (44) Yamakawa, H. *Modern Theory of Polymer Solutions*; Harper and Row: New York, 1977; pp 62–68.
- (45) Boudenne, N.; Anastasiadis, S. H.; Fytas, G.; Xenidou, M.; Hadjichristidis, N.; Semenov, A. N.; Fleischer, G. *Phys. Rev. Lett.* **1996**, *77*, 506. Anastasiadis, S. H.; Fytas, G.; Semenov, A. N.; Fleischer, G.; Xenidou, M.; Hadjichristidis, N. Manuscript in preparation.
- (46) Harville, S.; Chrissopoulou, K.; Anastasiadis, S. H.; Fytas, G.; Pispas, S.; Mays, J. W.; Hadjichristidis, N. Manuscript in preparation.

MA961735K